Ignition characteristics of dual-fuel methane-n-hexane-oxygen-diluent mixtures in a rapid compression machine and a shock tube

Yizhuo He[a,b], Yingdi Wang[a,b], Claire Grégoire[c], Urszula Niedzielska[c,d], Remy Mével[a,b,*], Joseph E. Shepherd[c,*]

[a]*Center for Combustion Energy, Tsinghua University, Beijing, China.*
[b]*Department of Automotive Engineering, Tsinghua University, Beijing, China.*
[c]*Graduate Aeronautical Laboratories, California Institute of Technology, Pasadena, USA*
[d]*Warsaw University of Technology, Warsaw, Poland*

Abstract

Ignition delay times of methane-n-hexane-oxygen mixtures were studied experimentally and numerically in a wide temperature range (640-2335 K) using both a rapid compression machine (RCM) and a shock tube (ST). The RCM results demonstrated a two-stage ignition and negative temperature coefficient (NTC) behavior. Increasing n-hexane concentration, pressure and equivalence ratio shortened the ignition delay time. For the ST experiments, the addition of 10% n-hexane (relative to methane) can reduce the ignition delay time dramatically. However, no further reduction effect can be achieved with increasing addition of n-hexane from 10% to 20%. In addition, increasing equivalence ratio reduces the effect of n-hexane addition on ignition delay time. Three detailed chemical mechanisms, CaltechMech, GalwayMech and LLNLMech, were evaluated based on a quantitative error analysis. LLNLMech and CaltechMech demonstrated the best performance in the RCM and ST temperature ranges, respectively. Chemical kinetic analyses showed that the addition of n-hexane to methane provides some chemical pathways not available for methane oxidation which result in the production of active radicals and eventually accelerate the ignition of the methane-oxygen mixtures. The crucial intermediate species for the ignition process are H_2O_2 and H under RCM and ST conditions, respectively.

*Corresponding author: mevel@mail.tsinghua.edu.cn

1. Introduction

A shortage of crude oil is expected within this century. In addition, air pollution is becoming more concerning and more stringent regulations on pollutant emissions from internal combustion engines are anticipated. The use of natural gas as a fuel for internal combustion engine (ICE) operating under diesel conditions is a promising approach for addressing these issues [1, 2].

Advantages of natural gas include vast and geographically widespread resources, as well as some relevant combustion parameters such as a high octane number, a high anti-knock capability and low pollutant emissions, leading to a substantial reduction in carbon dioxide emissions, and possibly of NOx and particulate matter as compared to diesel and gasoline fueled IC engines [3, 4, 5, 6]. On the other hand, natural gas has unfavorable combustion characteristics, such as a long ignition delay time, high auto-ignition temperature, low flame propagation speed for lean mixtures and poor lean burn capability. These can result in increased cycle-to-cycle variations, reduced thermal efficiency, and increased HC emission under fuel-lean conditions [7, 8, 9]. Consequently, a strategy to enhance ignition is needed to take advantage of the low emission of soot and NOx and the reduced formation of unburnt HC and CO possible with natural gas fueled IC engines. Pilot-ignited dual-fuel engines have proven to be a promising engine concept to improve and control the ignition of natural gas-air mixture under diesel conditions [2]. This strategy consists of triggering the ignition of a premixed charge using a micro-spray of diesel fuel [10, 11, 12, 13].

Properly optimized, the adoption of the pilot injection strategy would reduce the delay to the main ignition event, smoothen the premixed combustion phase, as well

as reduce noise and pollutant emissions at partial loads [14, 15, 16, 17]. However, because of the complexity of spray-induced ignition, substantial efforts are needed to optimize the combustion chamber geometry, the spray characteristics and the ignition strategies [18, 19, 20, 21, 22, 14, 23, 24]. In order to reducing the dependence on engine tests and to improving work efficiency, such an optimization process could be performed using Computational Fluid Dynamics (CFD) simulations, coupling the fluid mechanics and the appropriate chemical kinetic mechanism. It has been reported that the delay to ignition, the location of the ignition of the diesel spray, as well as the energy release rate characteristics are very sensitive to the content of methane in the methane-air pre-mixture [25, 4, 26, 18]. This indicates that the ignition process is very sensitive to the mixing process and to the chemical kinetics. Consequently, reliable chemical kinetic mechanisms are needed to support CFD simulations to optimizing this type of pilot-ignited dual-fuel engine. Regarding development and validation of chemical kinetic mechanisms, ignition delay time is widely considered as a combustion characteristic parameter of primary importance.

Given the complexity and variability of both natural gas and diesel composition, simple surrogate fuels should be employed to perform related chemical kinetic investigations. For natural gas, methane is generally considered as an appropriate surrogate. For diesel, a large number of surrogates have been proposed and may include up to 10 hydrocarbons [27]. The present study was carried out with n-hexane because it can be studied with room temperature starting conditions. While numerous experimental data on ignition are available for methane- [28, 29, 30] and n-hexane-based [31, 32, 33, 34, 35] mixtures, experimental data for dual-fuel methane-n-alkane mixtures are scarce. Liang et al. [36] studied the ignition delay-time of n-heptane-methane-based mixtures in a shock tube. The present study differs from that of Liang et al. in the approach used to prepare the mixtures. To determine the respective effects of methane and n-heptane, they replaced a fraction of methane by n-heptane whereas we have chosen to add a certain quantity of n-hexane to methane-oxygen-diluent mixtures of a given equivalence ratio. The present study also significantly extends the range of temperatures and pressures over which the

3

ignition of the dual-fuel mixtures is studied.

The objective of the present study was to investigate experimentally and numerically the impact of n-hexane addition on the ignition of methane. Due to its higher vapor pressure as compared to n-heptane, n-hexane was chosen as a diesel surrogate. We recognize that some of the physical properties of diesel are not captured when using a single alkane such as n-hexane since real diesel is a blend of hundred of hydrocarbons with carbon numbers in the range C_{10}-C_{24}, and a boiling temperature in the range 190-360 °C [37]. Studying real diesel requires to solve a number of technical difficulties including heating the experimental facilities and ensuring the thermal stability of the hydrocarbon-air mixtures [38]. A rapid compression machine (RCM) and a shock tube (ST) were employed to assess the ignition characteristics of dual-fuel methane-n-hexane-oxygen-diluent mixtures in a wide range of temperature and pressure. In addition, three detailed chemical kinetic mechanisms were evaluated. Chemical kinetic analyses were conducted to unravel the underlying ignition mechanism of methane-n-hexane mixtures.

2. Material and method

2.1. Rapid compression machine

The low- and intermediate-temperature (640-878 K) ignition experiments were performed using the Tsinghua University Rapid Compression Machine facility which detailed description is given in Di et al. [39].
The ignition delay time was defined as the time between the end of compression and the maximum pressure derivative. For two-stage ignition, the first-stage ignition was defined as the time between the end of compression and the first local maximum in the pressure derivative curve. The uncertainty on the delay time is estimated to be approximately 10-15%. A typical experimental pressure signal obtained during the RCM experiments is shown in Figure 1 (a).

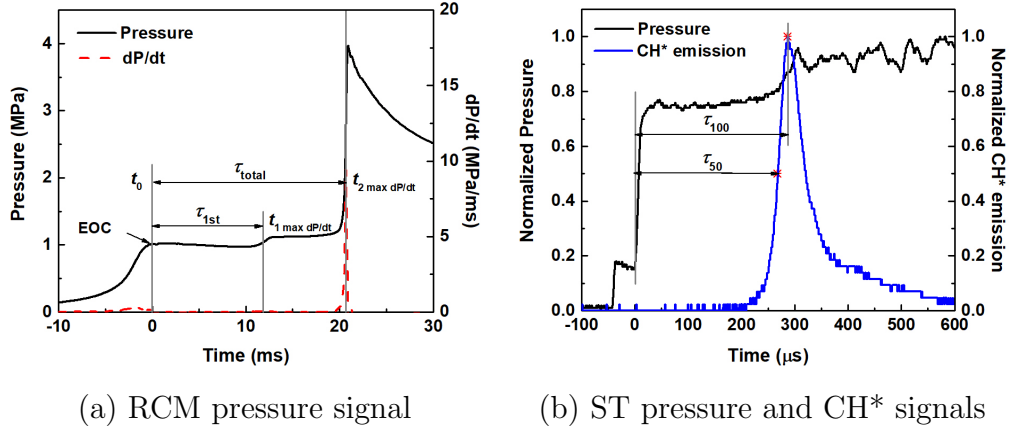(a) RCM pressure signal   (b) ST pressure and CH* signals

Figure 1: Typical experimental signals obtained using the RCM and ST facilities. (a): Mixture 1; P=2 MPa; T=670 K. (b) Mixture 14; P=415kPa; T=1353 K. EOC stands for end of compression

2.2. Shock tube

The high-temperature (1250-2335 K) ignition experiments were carried out using the Galcit 6-inch Shock Tube. A detailed description of the ST apparatus and diagnostics was previously given in [40, 41, 42]. The ignition event was studied behind reflected shock waves using OH*, CH*, and CO_2* emission. It was characterized using two times of reaction defined as: (i) the time to half emission maximum ($\tau_{50\%}$); and (ii) the time to the emission maximum ($\tau_{100\%}$). The uncertainty on the characteristic reaction times is estimated to be approximately 20%. Typical pressure and CH* emission signals obtained during the ST experiments are shown in Figure 1 (b).

2.3. Test mixtures

The reactive mixtures were prepared in a separate tank using the partial pressure method for both the RCM and the ST experiments. The tank of the RCM allowed mixtures to mix through diffusion for several hours before performing the experiments. A brushless fan was mounted inside the tank for the ST experiments, hence, approximately one or two hours were needed to ensure homogeneity. The residual pressure in both mixture tanks before mixture preparation was below 1 Pa. Ultra-high purity grade methane (99.999%), oxygen (99.999%), nitrogen (99.999%), argon (99.999%) and pure n-hexane (99%) were used for all the experiments. No

further purification was performed. The equivalence ratio was defined based on both the main fuel (ϕ_m) only and on the total amount of fuel (ϕ_t). ϕ_m is expressed as

$$\phi_m = \frac{X_{F_M}/X_{O_2}}{(X_{F_M}/X_{O_2})_{stoic}} \quad , \tag{1}$$

whereas ϕ_t is expressed as

$$\phi_t = \frac{2X_C + 0.5X_H}{X_O}. \tag{2}$$

The addition ratio of the additive fuel was defined as

$$R_A = \frac{X_{F_A}}{X_{F_M}}, \tag{3}$$

where X_{F_M} and X_{F_A} denote the amount of main fuel and additive fuel, respectively. F_M stands for methane and F_A stands for n-hexane except for Mixtures 14 to 16 for which n-hexane was the main fuel and methane was the added fuel. For RCM experiments, both nitrogen and argon were employed as diluent gas in order to extend the range of tested temperatures by altering the overall heat capacity. For the ST experiments, argon was used as the diluent gas to minimize the effect of vibrational relaxation and reflected shock wave bifurcation. The dilution ratio was selected to ensure the measured ignition delay times are in the appropriate ranges of observation times of the present RCM and ST facilities. Detailed mixture compositions and experimental conditions are summarized in Table 1.

Table 1: Experimental conditions and mixture compositions employed in the present work.

| Mixture | Mole Fraction (%) | | | | | ϕ_m | ϕ_t | T(K) | P(kPa) | Facility |
	n-C_6H_{14}	CH_4	O_2	N_2	Ar					
1	0.94	9.42	18.87	23.58	47.19	1.00	1.47	652-853	1000,2000	RCM
2	1.88	9.4	18.9	13.22	56.6	1.00	1.94	640-825	1000,2000	RCM
3	0.49	4.92	19.72	30.57	44.3	0.50	0.74	656-878	1000,2000	RCM
4	-	1	3	-	96	0.67	0.67	1630-2125	234-315	ST
5	-	1.33	2.67	-	96	1.00	1.00	1539-2335	233-297	ST
6	-	2	2	-	96	2.00	2.00	1666-2286	200-295	ST
7	0.1	1	3	-	95.9	0.67	0.98	1398-1723	306-386	ST
8	0.13	1.33	2.66	-	95.88	1.00	1.46	1510-1761	278-332	ST
9	0.2	2	2	-	95.8	2.00	2.95	1675-2156	219-294	ST
10	0.2	1.1	2.99	-	95.71	0.74	1.37	1455-1784	271-380	ST
11	0.26	-	3.74	-	96	0.66	0.66	1298-1474	320-377	ST
12	0.38	-	3.62	-	96	1.00	1.00	1298-1585	258-405	ST
13	0.7	-	3.3	-	96	2.02	2.02	1336-1606	308-392	ST
14	0.26	0.03	3.69	-	96.02	0.67	0.69	1247-1536	353-417	ST
15	0.38	0.04	3.62	-	95.96	1.00	1.02	1297-1479	340-402	ST
16	0.7	0.07	3.3	-	95.93	2.02	2.06	1368-1490	324-365	ST

2.4. Numerical modeling

Computational simulations were performed using the Senkin code [43] of the Chemkin II package [44] or Cantera [45], through a numerical procedure implemented in Matlab. Three state-of-the-art detailed reaction mechanisms were evaluated: (i) CaltechMech [46] (1159 reactions and 192 species), (ii) GalwayMech [32] (4150 reactions and 913 species), and (iii) LLNLMech [47] (2834 reactions and 661 species). The sub-mechanisms of the electronically excited species containing OH*, CH* and CO_2* [40] were added to each mechanism in order to reproducing ignition delay times measured by emission diagnostics in the ST. A constant volume reactor was used to predict the ignition delay times in shock tube. For the RCM experiments, the ignition delay time is long enough to be affected by heat losses after the end of the compression. Hence, a variable volume reactor model was employed as in [48]. A series of non-reactive experiments were performed in which oxygen was replaced by nitrogen to avoid ignition. These experiments enabled the determination of the equivalent specific volume profiles by measuring the pressure in the test section and assuming an adiabatic isentropic expansion process is taking place after the end of compression.

2.5. Evaluation of reaction model performance

In order to quantitatively evaluate the predictive capability of the three chemical kinetic mechanisms, a number of indicators have been calculated.

The relative error of the ith experimental data point (E_i) enables to evaluate the local performance of the models, that is for a single data point. It was calculated as

$$E_i = \frac{\tau^i_{model} - \tau^i_{expe}}{\tau^i_{expe}} \times 100 \qquad (4)$$

where τ^i_{expe} and τ^i_{model} are the experimental and numerical ignition delay time for the ith data point, respectively.

In order to evaluate the overall performance of the mechanisms, the mean and the maximum absolute errors were calculated. The expression of the mean absolute

error (μ) was

$$\mu = \frac{1}{N} \sum_{i=1}^{n} |E_i| \qquad (5)$$

where N is the total number of experimental data points. The maximum absolute error (E_{max}) was

$$E_{max} = max(|E_{i=1,...,N}|) \qquad (6)$$

A more detailed evaluation of the mechanisms performance, was obtained by calculating the distribution of relative error. Bins of 10% were employed. The relative population for the jth bin, RP_j, is expressed by

$$RP_j = \frac{n_j}{N} \qquad (7)$$

where n_j is the number of data points that conforms to

$$|E_j - v_j| < 5\% \qquad (8)$$

where v_j denotes the central value of the jth bin.

3. Results and discussion

3.1. Low- and intermediate-temperature ignition in RCM

3.1.1. Experimental results and reaction models performance

Figure 2 shows the effects of n-hexane concentration, pressure, and equivalence ratio on the ignition delay time of methane-n-hexane-oxygen-diluent mixtures. Two-stage ignition was observed for all mixtures and conditions within the temperature range 700-820 K and corresponds to a characteristic feature of the ignition of n-hexane-based mixtures. In addition, the negative temperature coefficient (NTC) behavior of the total ignition was observed in all the experimental conditions except for Mixture 2 at 2 MPa (shown in Figure 3(b)). This is because at higher pressure and n-hexane content, the NTC region is shifted beyond the accessible ranges of temperature and ignition delay time of our facility. The increase of n-hexane content from 10% to 20% dramatically shortens the first-stage and total ignition delay time by a factor of 3 to 4 over the temperature range studied (see Figure 2(a)). The increase of pressure from 1 to 2 MPa reduces the first-stage and total ignition delay

9

time by a factor of 2, and 3 to 5 for temperatures above 700 K, respectively. There is no evident effect of pressure for temperatures lower than 700 K (see Figure 2(b)). Equivalence ratio only affects the total ignition delay for temperature above 750 K with a decrease of approximately a factor of 2 as equivalence ratio is increased from 0.5 to 1 (see Figure 2(c)). It is noteworthy that the effects of pressure and equivalence ratio occur for temperatures above 700-750 K, whereas the effect of n-hexane addition on ignition delay time is observed over the entire temperature range. To underline the effect of fuel blending, we have calculated the adiabatic constant volume delay-time at P=1 MPa and T=745 K for a stoichiometric methane-oxygen-nitrogen-argon mixture and a stoichiometric n-hexane-oxygen-nitrogen-argon mixture. For these calculations performed with the LLNLMech, the dilution ratio was the same as for fuel-air mixtures and ratio X_{Ar}/X_{N2} was 4.28 as in our experiments. The delay-time for the methane-based mixture was 6.35 s, whereas the delay-time for the n-hexane-based mixture was 11.2 ms (3.1 ms for the first stage). These results should be interpreted with care because the calculated delay-time for the methane-based mixture is essentially extrapolated from a much higher temperature range over which methane combustion is typically studied. This indicates that, in the low-temperature range, the ignition characteristics of the most reactive fuel seem to dominate the ignition process of the dual-fuel mixture.

Figure 3 shows representative comparisons between the measured and predicted ignition delay times. Additional modeling results for the LLNLMech are shown in Figure 2. The three mechanisms reproduce the main trends experimentally measured but significant quantitative discrepancies are observed with relative error as high as 300% under certain conditions. Table 2 summarizes the performances of the mechanisms by presenting the mean and maximum absolute error on the first-stage and total ignition delay time. Overall, CaltechMech and GalwayMech overestimate both first-stage and total ignition delay time, especially below 725 K, while LLNLMech better predicts both the first-stage and total ignition with a mean absolute error on the first-stage and total ignition delay times of 64.58% and 24.35%, respectively.
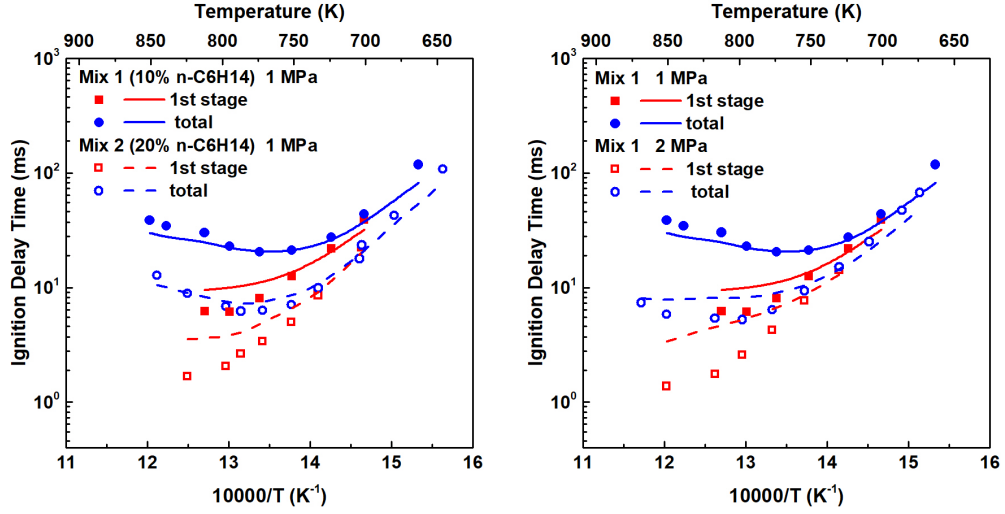
(a) Effect of n-hexane concentration   (b) Effect of pressure
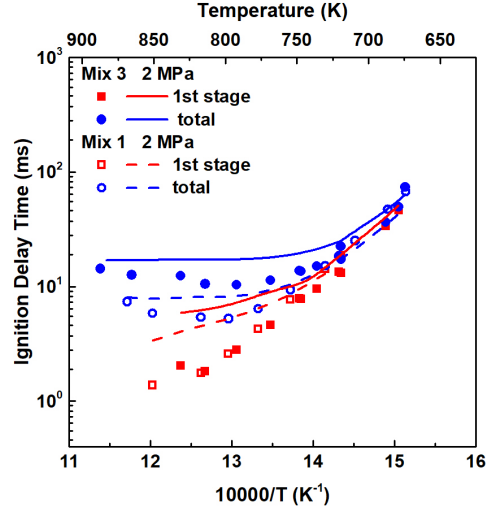
(c) Effect of equivalence ratio

Figure 2: Effect of n-hexane concentration (a), pressure (b) and equivalence ratio (c) on the first-stage and total ignition delay time of for CH_4-C_6H_{14}-O_2-diluent mixtures in a RCM. Lines correspond to the predictions of the LLNLMech.
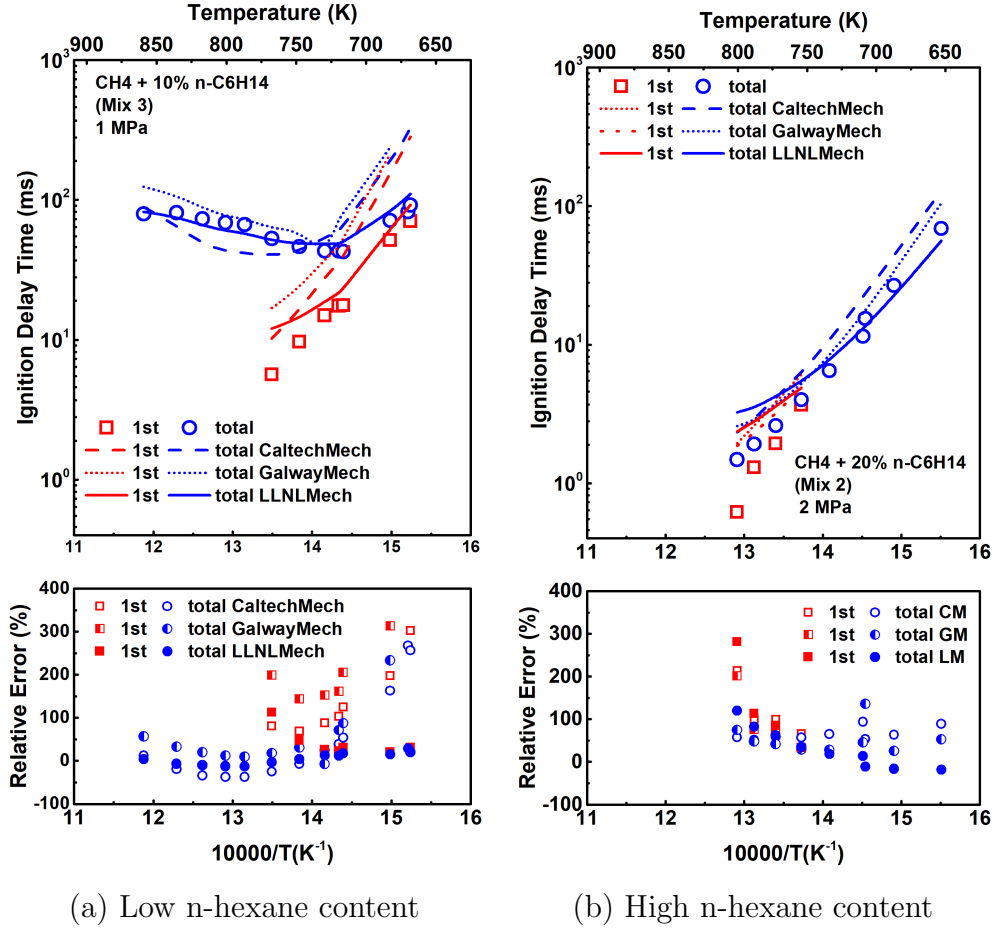
(a) Low n-hexane content   (b) High n-hexane content

Figure 3: Representative comparisons between the experimental and numerical first-stage and total ignition delay time for (a) Mixture 3 at 1 MPa and (b) Mixture 2 at 2 MPa in a RCM. In bottom plots, CM: CaltechMech; GM: GalwayMech; LM: LLNLMech.

Figure 4 shows the relative population (RP) of error for the first-stage and total ignition delay times. For first-stage ignition, the distribution of RP for all the mechanisms are centered on positive values which indicates an overall over-estimation. This implies that future work need to be focused on improving the predictive capability for first-stage ignition. As previously seen from the other quantitative indicators, LLNLMech demonstrates lower error. Concerning the total ignition delay, Caltech-Mech demonstrates a broad distribution whereas GalwayMech exhibits a distribution centered on approximately 50% error. Only LLNLMech exhibits a distribution of RP centered approximately on zero.
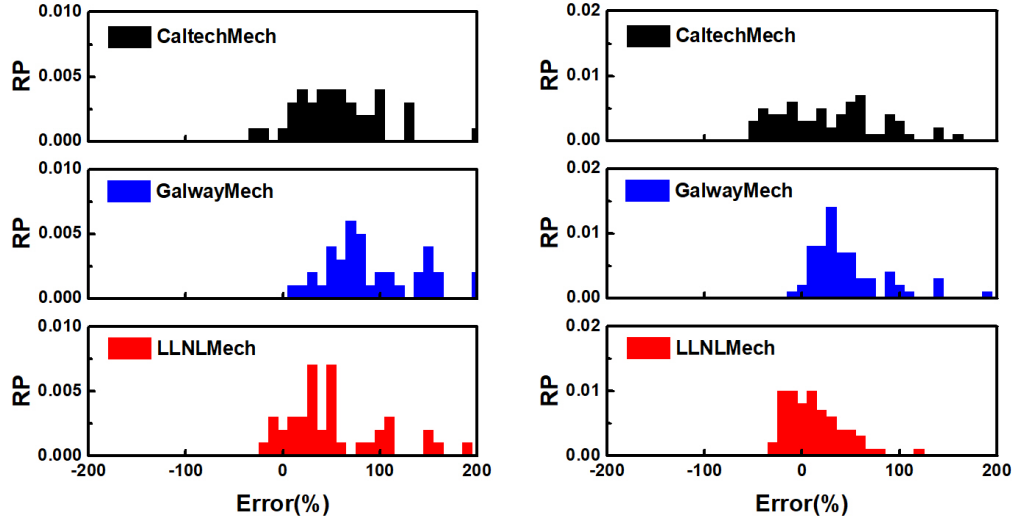
Table 2: Mean and maximum absolute error on the first-stage and total ignition delay time predicted by the three reaction models for CH_4-C_6H_{14}-O_2-diluent mixtures under RCM conditions.

Ignition delay time	CaltechMech		GalwayMech		LLNLMech	
	Mean %	Max %	Mean %	Max %	Mean %	Max %
First-stage	68.94	303.05	99.17	313.81	64.58	281.44
Total	47.39	268.00	48.72	233.32	24.35	119.75

*3.1.2. Chemical kinetic analyses*

Since the present work mainly focuses on the effect of n-hexane addition on the ignition delay time of methane-oxygen mixtures, chemical kinetic analyses were performed by comparing the modeling results between Mixture 1 (10% n-hexane) and Mixture 2 (20% n-hexane) at P=1 MPa and T=745 K. The temperature of 745 K was chosen because it is approximately the center of the temperature range investigated with the RCM and because, at this temperature, noticeable differences (approximately a factor of 3 for the total ignition delay) were observed between the delay times obtained for Mixtures 1 and 2. Due to its better performances at reproducing the RCM experimental data, the LLNLMech was employed for all the analyses.

The results of the sensitivity analysis performed on temperature are shown in Figure 5(a). It is noted that the sensitivity coefficients have been integrated over

(a) Error on first stage ignition delay (b) Error on total ignition delay

Figure 4: Relative population (RP) of relative error on (a) the first stage and (b) the total ignition delay time predicted by the three chemical kinetic mechanisms for CH_4-C_6H_{14}-O_2-diluent mixtures under RCM conditions.
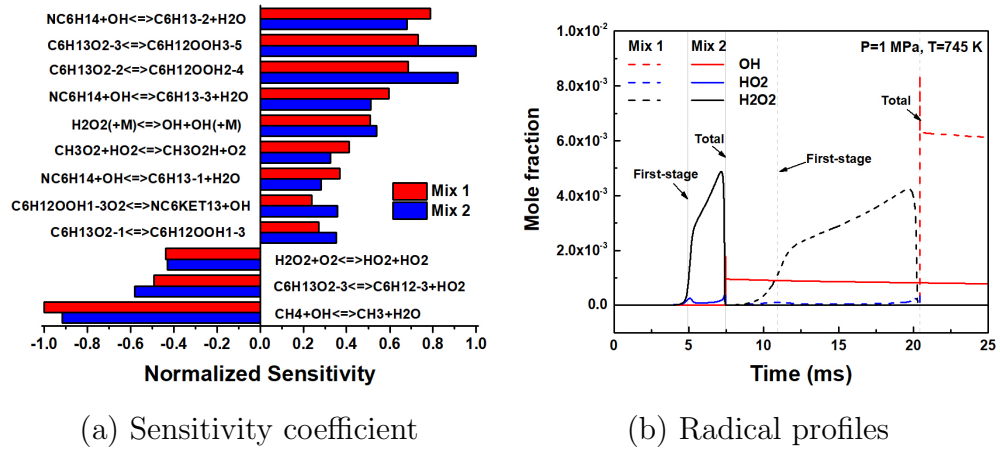
(a) Sensitivity coefficient (b) Radical profiles

Figure 5: Comparison of (a) the sensitivity coefficients on temperature and (b) OH, HO_2 and H_2O_2 mole fraction profiles between Mixture 1 (10% n-hexane) and Mixture 2 (20% n-hexane) at P=1 MPa and T=745 K. Calculations were performed with the LLNLMech.

the full time of the simulation. The sensitivity coefficient on temperature for the ith reaction is defined as

$$C_i = \frac{\partial \ln T}{\partial \ln k_i} = \frac{k_i}{T} \frac{\partial T}{\partial k_i}, \tag{9}$$

where k_i is the rate constant of reaction i. A positive coefficient indicates a reaction that promotes ignition, and a negative one indicates a reaction that delays ignition. The reactions which exhibit the highest positive coefficients are almost all related to the low-temperature oxidation of n-hexane. This demonstrates the primary influence of the n-hexane addition to the mixture on the ignition process. With the increase of n-hexane addition from 10 to 20%, the sensitivity coefficients for the isomerization reactions $C_6H_{13}O_2$-3 = $C_6H_{12}OOH3$-5 and $C_6H_{13}O_2$-2 = $C_6H_{12}OOH2$-4 increase and overcome that of the H abstraction reaction NC_6H_{14} + OH = C_6H_{13}-2 + H_2O. The sensitivity coefficients of isomerization reaction $C_6H_{13}O_2$-1 = $C_6H_{12}OOH1$-3 and its subsequent decomposition reaction $C_6H_{12}OOH1$-$3O_2$ = NC_6KET13 + OH also increase. The decomposition reaction H_2O_2 (+M) = OH + OH (+M) and the chain terminating reaction HO_2 + HO_2 = H_2O_2 + O_2 exhibit high sensitivity. This indicates that OH, HO_2, and H_2O_2 play critical roles in the ignition process of methane-oxygen mixture with n-hexane addition. Note that the species names we employed correspond to those used in the LLNLMech. We have provided the names and structures of these molecules as a supplemental material.

Figure 5(b) compares the OH, HO_2, and H_2O_2 profiles predicted for Mixture 1 (10% n-hexane) and Mixture 2 (20% n-hexane). There is an accumulation of H_2O_2 between the first-stage and total ignition delay time, and this is due to the conversion of HO_2 radical to H_2O_2 by HO_2 + HO_2 = H_2O_2 + O_2. Then, the decomposition of H_2O_2 generates a large amount of OH radical inducing the second-stage ignition. This chemical sequence explains the high sensitivity coefficient of these two reactions.

Figure 6 shows the rate of production (ROP) profiles for HO_2 and OH radicals production during the first-stage and total ignition for Mixture 1 (10% n-hexane) and Mixture 2 (20% n-hexane).

Concerning HO_2, before the first-stage ignition, the reactions of oxygen with HCO and CH_3O, which originate from the low-temperature n-hexane oxidation, initiate the production of HO_2 radical. Between the first-stage and total ignition delay time,

15

(a) HO_2 during first-stage ignition

(b) HO_2 during second-stage ignition

(c) OH during first-stage ignition

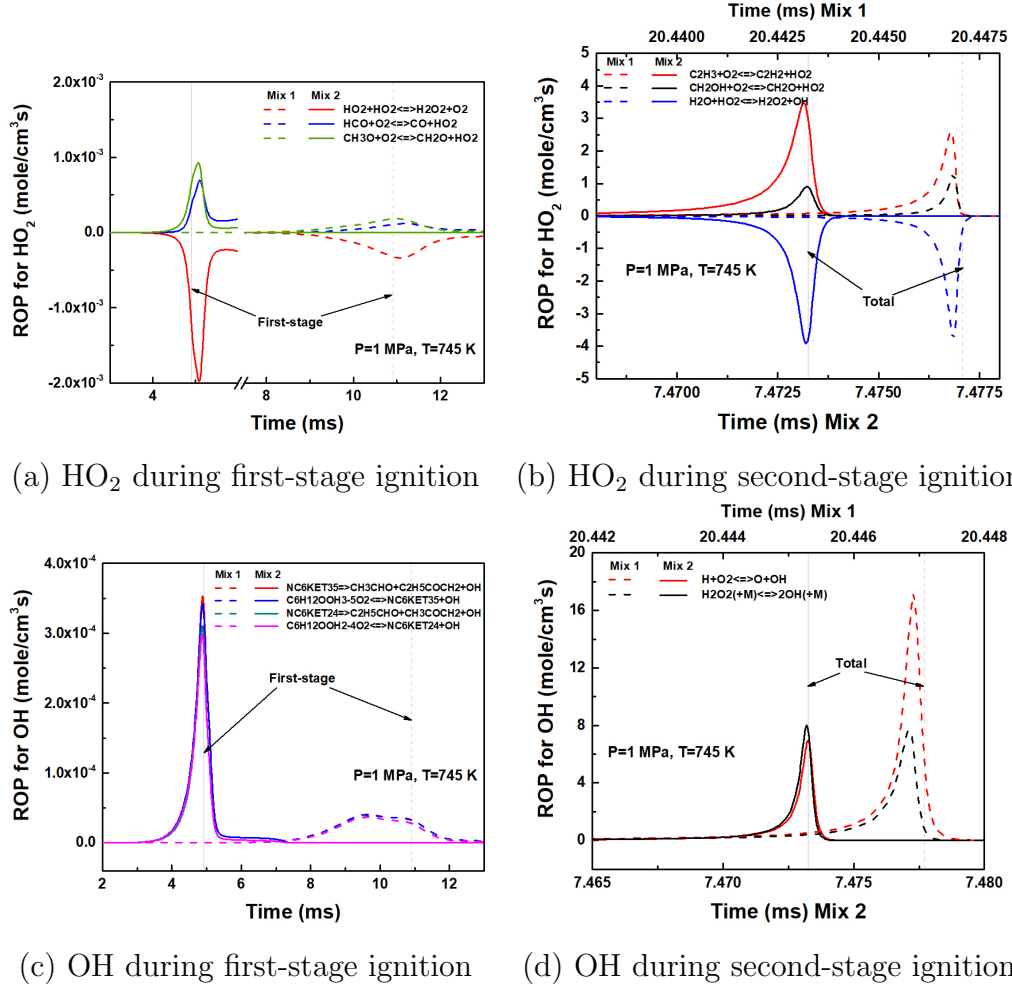
(d) OH during second-stage ignition

Figure 6: Comparison of the key reactions for HO_2 (a) (b) and OH (c) (d) radical production profiles during first-stage and second-stage ignition between Mixture 1 (10% n-hexane) and Mixture 2 (20% n-hexane) at P=1 MPa and T=745 K. Calculations were performed with the LLNLMech.

reactions between oxygen and C_2H_3, CH_2OH are responsible for the production of HO_2 radical. Simultaneously, a large amount of HO_2 radical is converted into H_2O_2 through $HO_2 + HO_2 = H_2O_2 + O_2$ and $HO_2 + H_2O = H_2O_2 + OH$. These explain the accumulation of H_2O_2 between the fist-stage and total ignition delay time. Besides, all the reactions abovementioned are enhanced by increasing the amount of n-hexane.

As for OH radical, during the first-stage ignition, the production of OH radical is mainly due to (i) the OH elimination reactions involving $C_6H_{12}OOH3\text{-}5O_2$ and $C_6H_{12}OOH2\text{-}4O_2$, and (ii) the decomposition reactions of NC_6KET35 and NC_6KET24. These latter reactions are the subsequent steps of the isomerization reactions and exhibit high sensitivity coefficient as previously mentioned. These four reactions are enhanced by the increased amount of n-hexane in the mixture. For total ignition, chain branching reaction $H + O_2 = O + OH$ and H_2O_2 decomposition reaction H_2O_2 $(+M) = OH + OH$ $(+M)$ dominate the production of OH radical. Moreover, the increasing addition of n-hexane from 10 to 20% promotes the OH radical production rate of H_2O_2 $(+M) = OH + OH$ $(+M)$ which overcomes that of $H + O_2 = O + OH$.

We also performed an analysis of the rate of production for CH_4. The results of this analysis are shown in Figure 7. During the first ignition stage, the consumption of CH_4 is only due to $CH_4+OH=CH_3+H_2O$. During the second ignition stage, the consumption of methane is distributed between $CH_4+OH=CH_3+H_2O$ and $CH_4+H=CH_3+H_2$.

Based on the sensitivity and rate of production analyses performed, the effect of n-hexane addition on the ignition delay time of methane-oxygen mixtures is due to the low-temperature chemistry of n-hexane. Chemical pathways not available for methane oxidation become more and more important as n-hexane content is increased and result in the production of active radicals, mainly OH, which accelerates the ignition of the methane-oxygen mixtures. More precisely, the main chemical sequences responsible for the first-stage ignition are $C_6H_{13}O_2\text{-}3 \rightarrow C_6H_{12}OOH3\text{-}5 \rightarrow C_6H_{12}OOH3\text{-}5O_2 \rightarrow NC_6KET35$ and $C_6H_{13}O_2\text{-}2 \rightarrow C_6H_{12}OOH2\text{-}4 \rightarrow C_6H_{12}OOH2\text{-}$

17

$4O_2 \rightarrow NC_6KET24$; while the decomposition of H_2O_2 is responsible for the second-stage ignition.

(a) First-stage ignition   (b) Second-stage ignition
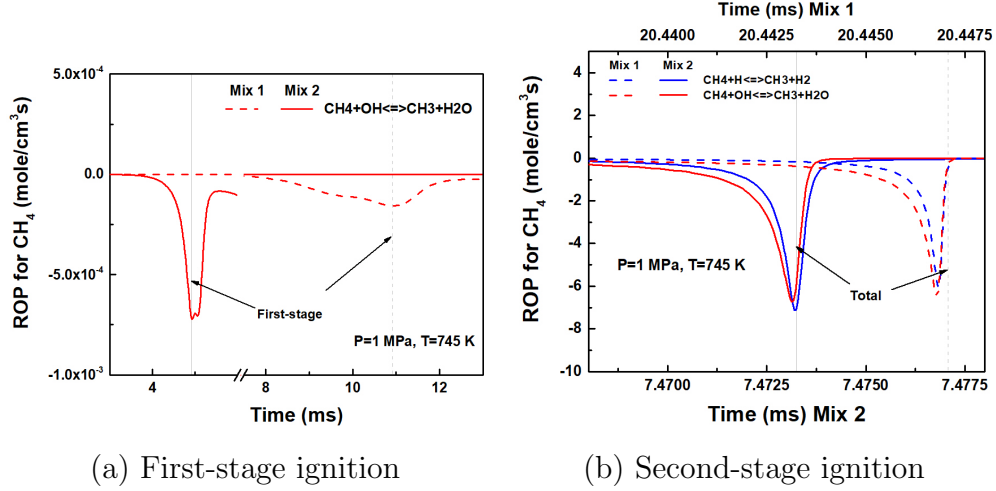
Figure 7: Comparison of the key reactions for CH_4 during first-stage and second-stage ignition between Mixture 1 (10% n-hexane) and Mixture 2 (20% n-hexane) at P=1 MPa and T=745 K. Calculations were performed with the LLNLMech.

3.2. High-temperature ignition in ST

3.2.1. Experimental results and reaction models performance

Figure 8 to 10 show the ignition delay times obtained in ST based on OH* as well as comparisons with the predictions of the three chemical kinetic mechanisms. Results based on CH* and CO_2* are provided in the supplementary material.

Methane exhibits much longer ignition delay times than n-hexane, which is in accordance with previous experimental data [49]. With respect to the methane-n-hexane mixtures, the ignition delay time decreases as temperature increases and no negative temperature coefficient behavior was observed in current high-temperature range. There is a distinguishable effect caused by the addition of 10% n-hexane, which shortens the ignition delay time dramatically. It is compelling that a sharp decrease by a factor of 5 to 7 was observed under fuel-lean conditions. Nevertheless, no further influence can be exerted in reducing the ignition delay time when increasing the addition of n-hexane from 10% to 20% as shown in Figure 8. From a different
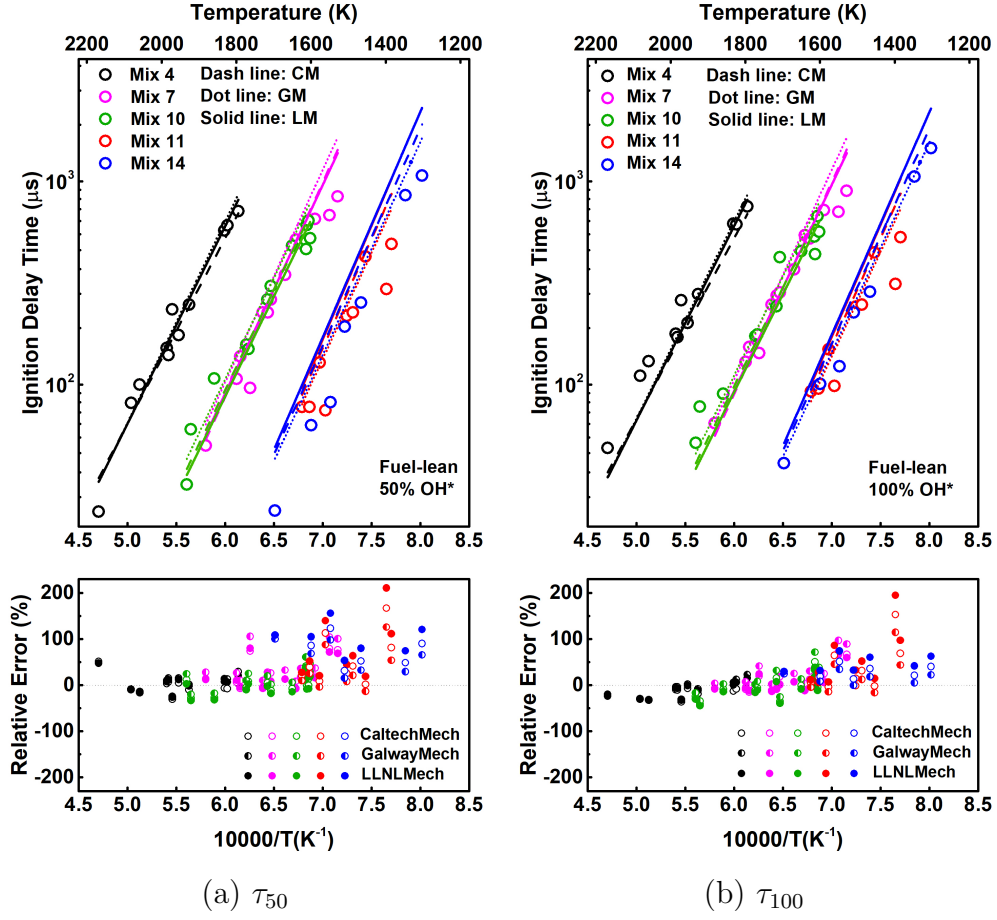
18

Figure 8: Comparisons between the experimental and numerical ignition delay time based on OH* emissions for lean CH_4-C_6H_{14}-O_2-diluent mixtures. CM: CaltechMech model; GM: GalwayMech; LM: LLNLMech.

perspective, comparing the n-hexane with and without methane addition, it is noteworthy that no perceptible effect can be achieved by the addition of 10% methane to n-hexane. These imply that n-hexane with high reactivity overwhelmingly dominates the ignition characteristics of methane-n-hexane mixtures when it exceeds a certain amount. Regarding the effect of equivalence ratio, the effect of n-hexane addition in shortening the ignition delay time weakens for stoichiometric and rich mixtures, see Figure 9 and 10. This can be attributed to the self-inhibition property of hydrocarbons on the ignition process in the high-temperature range [40, 31].
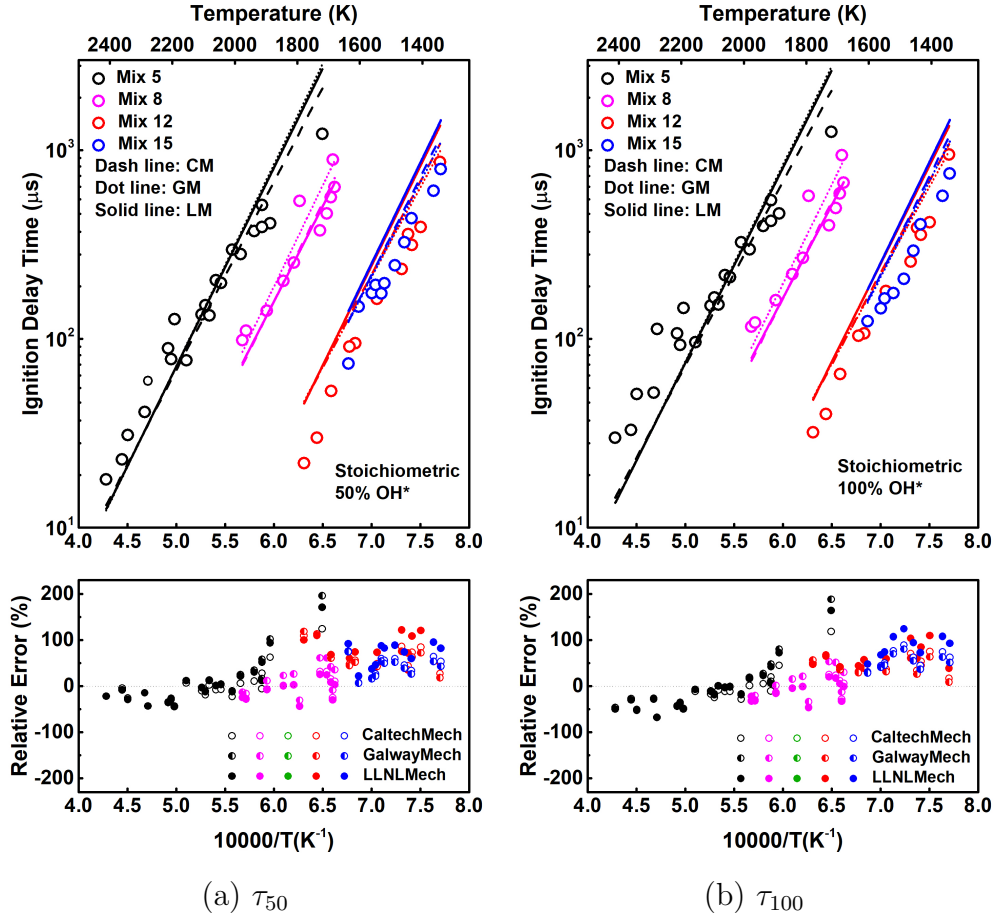

(a) τ_{50} (b) τ_{100}

Figure 9: Comparisons between the experimental and numerical ignition delay time based on OH* emissions for stoichiometric CH_4-C_6H_{14}-O_2-diluent mixtures. CM: CaltechMech model; GM: GalwayMech; LM: LLNLMech.
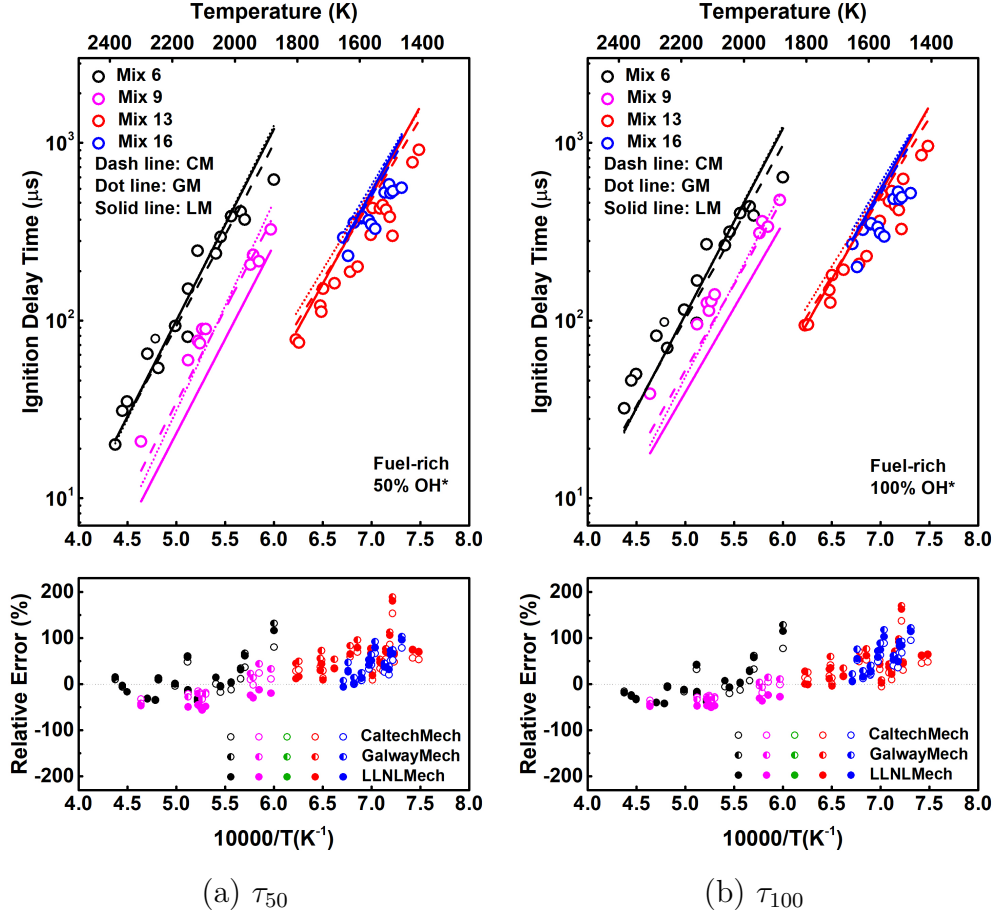
Figure 10: Comparisons between the experimental and numerical ignition delay time based on OH* emissions for rich CH_4-C_6H_{14}-O_2-diluent mixtures. CM: CaltechMech model; GM: GalwayMech; LM: LLNLMech.

Table 3: Mean and maximum absolute error on the high-temperature ignition delay time predicted by the three reaction models under ST conditions for CH_4-C_6H_{14}-O_2-Ar mixtures.

	CaltechMech		GalwayMech		LLNLMech	
	Mean %	Max %	Mean %	Max %	Mean %	Max %
Ignition delay time	32.61	166.76	37.67	196.14	41.196	210.77

All three chemical kinetic mechanisms capture the main experimental features but significant deviations can be observed with relative error as high as 200% under certain conditions. Overall, GalwayMech and LLNLMech overestimate the ignition delay time more than CaltechMech, especially for mixtures with n-hexane under

stoichiometric and fuel-rich conditions. Table 3 demonstrates the predictive performance of the three mechanisms by listing the mean and maximum absolute error on the measured ignition delay times of all the 13 mixtures based on OH*, CH* and CO_2* emission diagnostics. CaltechMech exhibits a better predictive capability of the high-temperature ignition delay time with a mean absolute error of 32.61%. Figure 11 shows the relative population of relative error for the ignition delay time and it can be seen that CaltechMech exhibits a distribution of RP centered much closer to zero as compared to the other two mechanisms.
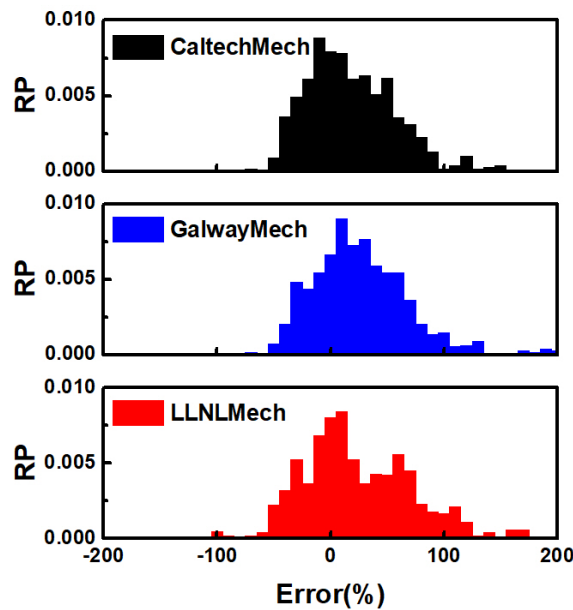

Figure 11: Relative population (RP) of relative error on ignition delay time in shock tube predicted by the three chemical kinetic mechanisms for CH_4-C_6H_{14}-O_2-Ar mixtures under ST conditions.

3.2.2. Chemical kinetic analyses

In order to gain further insight into the effect of n-hexane addition on the ignition of methane-oxygen mixtures at high temperature, chemical kinetic analyses were conducted for Mixture 5 (methane) and Mixture 8 (methane and 10% n-hexane) at P=0.3 MPa and T=1700 K. This temperature was chosen because it corresponds approximately to the lowest and highest temperature for the experiments performed with methane and n-hexane as the only fuel, respectively. Due to its higher performance in reproducing the ST data, CaltechMech was adopted to perform these

analyses of the effect of n-hexane addition on high-temperature ignition delay time.
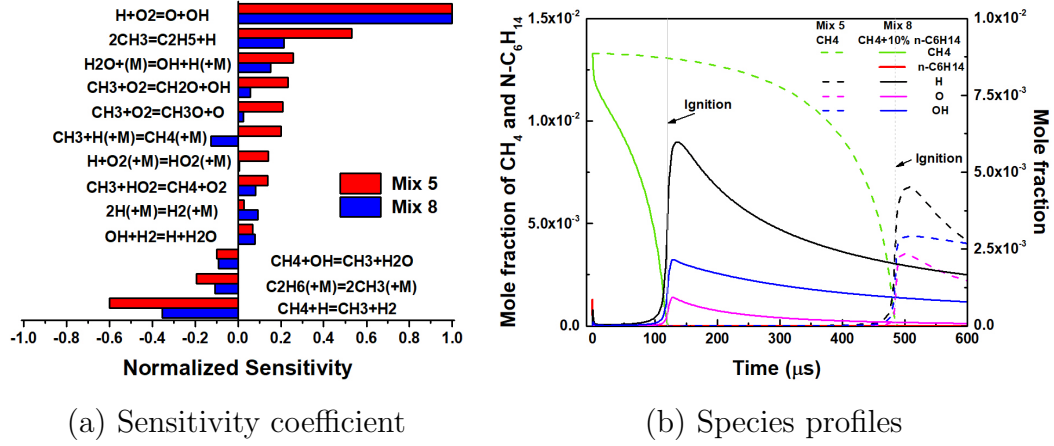

(a) Sensitivity coefficient

(b) Species profiles

Figure 12: Comparison (a) of the sensitivity coefficients on temperature and (b) of the H, O, OH, CH_4, and n-C_6H_{14} mole fraction profiles between Mixture 5 (methane) and Mixture 8 (methane and 10% n-hexane) at P=0.3 MPa and T=1700 K. Calculations were performed with the CaltechMech.

The normalized sensitivity coefficients on temperature (see Equation 9) are compared in Figure 12 (a). It is noted that the sensitivity coefficients have been integrated over the full time of the simulation. For both conditions, the chain branching reaction H + O_2 = O + OH exhibits an overwhelmingly high positive sensitivity coefficient due to its critical role in inducing the ignition. For all the CH_4- and CH_3-related reactions, either with positive or negative sensitivity coefficients, the sensitivity coefficients decrease dramatically when 10% n-hexane is added. The coefficient even changes from positive to negative for reaction CH_3 + H (+M) = CH_4 (+M). These imply that the n-hexane addition weakens the influence of methane on the ignition process. Besides, the sensitivity coefficients of H-related reactions 2H (+M) = H_2 (+M) and OH + H_2 = H + H_2O are increased by the n-hexane addition. Figure 12 (b) compares the H, O, OH, CH_4 and n-C_6H_{14} mole fraction profiles between Mixture 5 (methane) and Mixture 8 (methane and 10% n-hexane). Both the time scale and the evolution of the species profiles are quite different for the two mixtures. For Mixture 5, the concentration of methane decreases very slowly during the initial stage of the reaction and most of methane is consumed at a time close to ignition as the rate of methane removal becomes faster and faster. For Mixture 8, an initial rapid drop of the methane mole fraction is observed as n-hexane is

decomposed within few μs. The rate of methane consumption then decreases for approximately 50 μs and finally, increases again as the concentration of active radicals starts to increase just before ignition is taking place. Concerning the radical pool, the n-hexane addition induces a rapid production of H, O and OH radicals during the initial stage of the ignition process which is not observed for Mixture 5. In addition, the addition of n-hexane induces an increase of the peak concentration of H atom and a decrease of the peak concentration of O and OH. These imply the prominent importance of the rapid decomposition of n-hexane in producing active radicals, especially H, to accelerate the ignition of methane-oxygen mixtures.

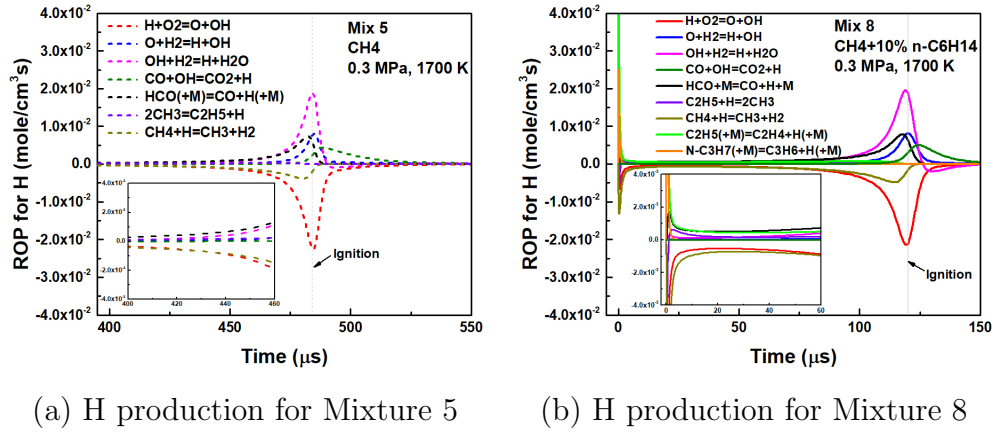(a) H production for Mixture 5　　(b) H production for Mixture 8

Figure 13: Comparison of the key reactions for H production and consumption during the ignition process between (a) Mixture 5 (methane) and (b) Mixture 8 (methane and 10% n-hexane) at P=0.3 MPa and T=1700 K. Calculations were performed with the CaltechMech.

Since the addition of n-hexane induces an increase of the peak concentration of H atom whereas that of O and OH decrease, rate of production analyses for H have been performed as shown in Figure 13. Without n-hexane addition, H radical production is initiated after several hundred microseconds. The main reactions which are responsible for H production before the chain branching reactions are activated correspond to HCO (+M) = H + CO (+M) and OH + H_2 = H + H_2O. The species HCO and H_2 originate from the slow oxidation sequence of methane, $CH_4 \rightarrow CH_3 \rightarrow CH_2O \rightarrow$ HCO. However, with n-hexane addition, H radical is produced rapidly at the initial stage through the decomposition reactions C_2H_5 (+M) = C_2H_4 + H (+M) and N-C_3H_7 (+M) = C_3H_6 + H (+M). The species C_2H_5 and N-C_3H_7 originate

24

from the rapid decomposition of n-hexane. This early production of active radicals readily triggers H-abstraction reaction on CH_4 and as a consequence accelerates the oxidation sequence mentioned above. This results in a continuous production of H radicals by HCO decomposition and eventually triggers the ignition via the typical chain branching mechanism $H + O_2 = O + OH$ and $O + H_2 = H + OH$. Hence, it can be concluded that reduction of the ignition delay time by n-hexane is largely due to the rapid decomposition of n-hexane at initial stage which produces H atom.

4. Conclusion

In the present study, the ignition characteristics of dual-fuel methane-n-hexane-oxygen-diluent mixtures were experimentally and numerically studied over wide ranges of temperature and pressure using a RCM and a ST.

The RCM results show that the two-stage ignition occurs within the temperature range 700-820 K. In addition, the typical NTC behavior of the total ignition was observed. The increase of n-hexane addition, pressure and equivalence ratio shortened the ignition delay time dramatically. In the ST experiments, the addition of 10% n-hexane (relative to methane) results in a substantial reduction of ignition delay time under fuel-lean conditions but no further reduction was observed with a larger amount of n-hexane addition (20%). The increase of equivalence ratio weakens the effect of n-hexane addition on shortening the ignition delay time.

Three detailed chemical kinetic mechanisms were evaluated based on a quantitative analysis. LLNLMech and CaltechMech demonstrate the best agreement with the experimental data obtained in the RCM and ST, respectively. Chemical kinetic analyses showed that under RCM conditions, the low-temperature chemistry of n-hexane induces OH radical formation through the decomposition of H_2O_2, which plays a critical role during the ignition process. Under ST conditions, the prompt decomposition of n-hexane results in an early production of active radicals, especially H radical, which accelerates the ignition through typical chain branching mechanism. The large variations of the ignition delay time with the changes of n-hexane addition and equivalence ratio explain the large variation observed previously in the delay and location of the ignition during methane-based mixtures piloted-ignition experiments.

In order to minimize cycle-to-cycle variation of micro-spray ICE, initial conditions before injection as well as the spray dynamics need to be accurately controlled to limit the local variation of composition in the combustion chamber.

Future work should focus on developing a reduced reaction model which combines the low-temperature LLNLMech and high-temperature CaltechMech mechanisms for integration in realistic numerical simulations of micro-spray ICE for optimizing the design of the injector and the geometry of the combustion chamber. In addition, experimental data for hydrocarbon fuel blends more representative of diesel are needed.

Acknowledgments

References

[1] L. Ma, J. Geng, W. Li, P. Liu, Z. Li, The development of natural gas as an automotive fuel in china, Energy Policy 62 (2013) 531 – 539.
URL http://www.sciencedirect.com/science/article/pii/S0301421513005739

[2] T. Korakianitis, A. Namasivayam, R. Crookes, Natural-gas fueled spark-ignition (SI) and compression-ignition (CI) engine performance and emissions, Progress in Energy and Combustion Science 37 (1) (2011) 89 – 112.
URL http://www.sciencedirect.com/science/article/pii/S0360128510000377

[3] A. Yousefi, M. Birouk, B. Lawler, A. Gharehghani, Performance and emissions of a dual-fuel pilot diesel ignition engine operating on various premixed fuels, Energy Conversion and Management 106 (2015) 322 – 336.
URL http://www.sciencedirect.com/science/article/pii/S0196890415009012

[4] S. Schlatter, B. Schneider, Y. Wright, K. Boulouchos, Experimental study of ignition and combustion characteristics of a diesel pilot spray in a lean premixed methane/air charge using a rapid compression expansion machine, in: SAE 2012 World Congress & Exhibition, SAE International, 2012.
URL https://doi.org/10.4271/2012-01-0825

[5] H. M. Cho, B.-Q. He, Spark ignition natural gas engines-A review, Energy Conversion and Management 48 (2) (2007) 608 – 618.
URL http://www.sciencedirect.com/science/article/pii/S0196890406001919

[6] J. Naber, D. Siebers, S. D. Julio, C. Westbrook, Effects of natural gas composition on ignition delay under diesel conditions, Combustion and Flame 99 (2) (1994) 192 – 200.
URL http://www.sciencedirect.com/science/article/pii/0010218094901228

[7] Y. Zhang, Z. Huang, L. Wei, J. Zhang, C. K. Law, Experimental and modeling study on ignition delays of lean mixtures of methane, hydrogen, oxygen, and argon at elevated pressures, Combustion and Flame 159 (3) (2012) 918 – 931.
URL http://www.sciencedirect.com/science/article/pii/S0010218011002951

[8] M. Y. Selim, Effect of engine parameters and gaseous fuel type on the cyclic variability of dual fuel engines, Fuel 84 (7) (2005) 961 – 971.
URL http://www.sciencedirect.com/science/article/pii/S0016236104003679

[9] F. Egolfopoulos, P. Cho, C. Law, Laminar flame speeds of methane-air mixtures under reduced and elevated pressures, Combustion and Flame 76 (3) (1989) 375 – 391.
URL http://www.sciencedirect.com/science/article/pii/0010218089901193

[10] L. Wei, P. Geng, A review on natural gas/diesel dual fuel combustion, emissions and performance, Fuel Processing Technology 142 (2016) 264 – 278.
URL http://www.sciencedirect.com/science/article/pii/S0378382015301715

[11] A. Shah, S. S. Thipse, A. Tyagi, S. D. Rairikar, K. P. Kavthekar, N. V. Marathe, P. Mandloi, Literature review and simulation of dual fuel diesel-CNG engines, in: SAE Technical Paper, The Automotive Research Association of India, 2011.
URL https://doi.org/10.4271/2011-26-0001

[12] R. Papagiannakis, D. Hountalas, Combustion and exhaust emission characteristics of a dual fuel compression ignition engine operated with pilot diesel fuel and natural gas, Energy Conversion and Management 45 (18) (2004) 2971 – 2987.
URL http://www.sciencedirect.com/science/article/pii/S0196890404000330

[13] M. Mbarawa, B. E. Milton, R. T. Casey, Experiments and modelling of natural gas combustion ignited by a pilot diesel fuel spray, International Journal of Thermal Sciences 40 (10) (2001) 927 – 936.
URL http://www.sciencedirect.com/science/article/pii/S1290072901012790

[14] X. Huang, F. Yang, M. Ouyang, Performance and emission optimization of pilot ignited natural gas diesel engine with single and dual injection pilot strategies and mbc toolkit, in: SAE Technical Paper, SAE International, 2015.
URL https://doi.org/10.4271/2015-01-1985

[15] P. Federico, D. Sahoo, P. Miles, R. Reitz, Modeling the ignitability of a pilot injection for a diesel primary reference fuel: Impact of injection pressure, ambient temperature and injected mass, SAE International Journal of Fuels and Lubricants 7 (1) (2014) 48–64.
URL http://www.jstor.org/stable/26273059

[16] J. Liu, F. Yang, H. Wang, M. Ouyang, S. Hao, Effects of pilot fuel quantity on the emissions characteristics of a CNG/diesel dual fuel engine with optimized pilot injection timing, Applied Energy 110 (2013) 201 – 206.
URL http://www.sciencedirect.com/science/article/pii/S0306261913002201

[17] G. A. Alla, H. Soliman, O. Badr, M. A. Rabbo, Effect of injection timing on the performance of a dual fuel engine, Energy Conversion and Management 43 (2) (2002) 269 – 277.
URL http://www.sciencedirect.com/science/article/pii/S0196890400001680

[18] J. Zheng, J. Wang, Z. Zhao, D. Wang, Z. Huang, Effect of equivalence ratio on combustion and emissions of a dual-fuel natural gas engine ignited with diesel, Applied Thermal Engineering 146 (2019) 738 – 751.
URL http://www.sciencedirect.com/science/article/pii/S1359431118339875

[19] A. Yousefi, H. Guo, M. Birouk, An experimental and numerical study on diesel injection split of a natural gas/diesel dual-fuel engine at a low engine load, Fuel 212 (2018) 332 – 346.
URL http://www.sciencedirect.com/science/article/pii/S001623611731298X

[20] J. M. S. Mattson, C. Langness, C. Depcik, An analysis of dual-fuel combustion of diesel with compressed natural gas in a single-cylinder engine, in: SAE Technical Paper, SAE International, 2018.
URL https://doi.org/10.4271/2018-01-0248

[21] S. Weber, R. Stegmann, M. Prager, G. Wachtmeister, The effect of inlet valve timing and engine speed on dual fuel NG-diesel combustion in a large bore engine, SAE International Journal of Engines 11 (2018) 229–246.
URL https://doi.org/10.4271/03-11-02-0015

[22] Z. Wang, Z. Zhao, D. Wang, M. Tan, Y. Han, Z. Liu, H. Dou, Impact of pilot diesel ignition mode on combustion and emissions characteristics of a diesel/natural gas dual fuel heavy-duty engine, Fuel 167 (2016) 248 – 256.
URL http://www.sciencedirect.com/science/article/pii/S0016236115012338

[23] H. K. Suh, Investigations of multiple injection strategies for the improvement of combustion and exhaust emissions characteristics in a low compression ratio (CR) engine, Applied Energy 88 (12) (2011) 5013 – 5019.
URL http://www.sciencedirect.com/science/article/pii/S0306261911004387

[24] R. Papagiannakis, D. Hountalas, C. Rakopoulos, Theoretical study of the effects of pilot fuel quantity and its injection timing on the performance and emissions of a dual fuel diesel engine, Energy Conversion and Management 48 (11) (2007) 2951 – 2961.
URL http://www.sciencedirect.com/science/article/pii/S0196890407002129

[25] A.-H. Kakaee, A. Paykani, M. Ghajar, The influence of fuel composition on the combustion and emission characteristics of natural gas fueled engines, Renewable and Sustainable Energy Reviews 38 (2014) 64 – 78.
URL http://www.sciencedirect.com/science/article/pii/S1364032114004055

[26] B. Sahoo, N. Sahoo, U. Saha, Effect of engine parameters and type of gaseous fuel on the performance of dual-fuel gas diesel engines-A critical review, Renewable and Sustainable Energy Reviews 13 (6) (2009) 1151 – 1184.
URL http://www.sciencedirect.com/science/article/pii/S1364032108001020

[27] C. Mueller, W. Cannella, T. Bruno, B. Bunting, H. Dettman, J. Franz, M. Huber, M. Natarajan, W. Pitz, M. Ratcliff, K. Wright, Methodology for formulating diesel surrogate fuels with accurate compositional, ignition-quality, and volatility characteristics, Energy & Fuels 26 (6) (2012) 3284–3303.

[28] U. Burke, K. P. Somers, P. O'Toole, C. M. Zinner, N. Marquet, G. Bourque, E. L. Petersen, W. K. Metcalfe, Z. Serinyel, H. J. Curran, An ignition delay and kinetic modeling study of methane, dimethyl ether, and their mixtures at high pressures, Combustion and Flame 162 (2) (2015) 315 – 330.
URL http://www.sciencedirect.com/science/article/pii/S001021801400251X

[29] J. M. Simmie, Detailed chemical kinetic models for the combustion of hydrocarbon fuels, Progress in Energy and Combustion Science 29 (6) (2003) 599 – 634.
URL http://www.sciencedirect.com/science/article/pii/S0360128503000601

[30] L. Spadaccini, M. Colket, Ignition delay characteristics of methane fuels, Progress in Energy and Combustion Science 20 (5) (1994) 431 – 460.
URL http://www.sciencedirect.com/science/article/pii/0360128594900116

[31] R. Mével, U. Niedzielska, J. Melguizo-Gavilanes, S. Coronel, J. E. Shepherd, Chemical kinetics of n-hexane-air atmospheres in the boundary layer of a moving hot sphere, Combustion Science and Technology 188 (11-12) (2016) 2267–2283.
URL https://doi.org/10.1080/00102202.2016.1211886

[32] K. Zhang, C. Banyon, C. Togbé, P. Dagaut, J. Bugler, H. J. Curran, An experimental and kinetic modeling study of n-hexane oxidation, Combustion and Flame 162 (11) (2015) 4194 – 4207.
URL http://www.sciencedirect.com/science/article/pii/S0010218015002576

[33] R. Mével, K. Chatelain, P. Boettcher, G. Dayma, J. Shepherd, Low temperature oxidation of n-hexane in a flow reactor, Fuel 126 (2014) 282 – 293.
URL http://www.sciencedirect.com/science/article/pii/S0016236114002208

[34] D. Davidson, S. Ranganath, K.-Y. Lam, M. Liaw, Z. Hong, Ignition delay time measurements of normal alkanes and simple oxygenates, Journal of Propulsion and Power 26 (2) (2010) 280–287.

[35] V. Zhukov, V. Sechenov, A. Starikovskii, Ignition delay times in lean n-hexane-air mixture at high pressures, Combustion and Flame 136 (1) (2004) 257 – 259.
URL http://www.sciencedirect.com/science/article/pii/S0010218003002517

[36] J. Liang, Z. Zhang, G. Li, Q. Wan, L. Xu, S. Fan, Experimental and kinetic studies of ignition processes of the methane-n-heptane mixtures, Fuel 235 (2019) 522–529.

[37] J. Farrell, N. Cernansky, F. Dryer, C. Law, D. Friend, C. Hergart, R. McDavid, A. Patel, C. Mueller, H. Pitsch, Development of an experimental database and kinetic models for surrogate diesel fuels, SAE Technical Paper (2007), # 2007-01-0201.

[38] R. Mevel, F. Rostand, D. Lemarie, L. Breyton, J.E. Shepherd, Oxidation of n-hexane in the vicinity of the auto-ignition temperature, Fuel 236 (2019) 373–381.

[39] H. Di, X. He, P. Zhang, Z. Wang, M. S. Wooldridge, C. K. Law, C. Wang, S. Shuai, J. Wang, Effects of buffer gas composition on low temperature ignition of iso-octane and n-heptane, Combustion and Flame 161 (10) (2014) 2531 – 2538.
URL http://www.sciencedirect.com/science/article/pii/S0010218014001242

[40] K. Chatelain, R. Mével, S. Menon, G. Blanquart, J. Shepherd, Ignition and chemical kinetics of acrolein-oxygen-argon mixtures behind reflected shock waves, Fuel 135 (2014) 498 – 508.
URL http://www.sciencedirect.com/science/article/pii/S0016236114006449

[41] R. Mével, J. E. Shepherd, Ignition delay-time behind reflected shock waves of small hydrocarbons-nitrous oxide(-oxygen) mixtures, Shock Waves 25 (2015) 217–229.

[42] R. Mével, K. Chatelain, G. Blanquart, J. Shepherd, An updated reaction model for the high-temperature pyrolysis and oxidation of acetaldehyde, Fuel 217 (2018) 226–239.

[43] A. Lutz, R. Kee, J. Miller, Senkin : a fortran program for predicting homogeneous gas phase chemical kinetics with sensitivity analysis, Tech. Rep. Sand87-8248, Sandia International Laboratories (1992).

[44] R. Kee, F. Rupley, J. Miller, Chemkin II : A fortran chemical kinetics package for the analysis of gas phase chemical kinetics, Tech. Rep. Sand89-8009B, Sandia International Laboratories (1993).

[45] D. Goodwin, H. Moffat, R. Speth, Cantera: An object-oriented software toolkit

for chemical kinetics, thermodynamics, and transport processes, `http://www.cantera.org`, version 2.2.0 (2015).

[46] G. Blanquart, P. Pepiot-Desjardins, H. Pitsch, Chemical mechanism for high temperature combustion of engine relevant fuels with emphasis on soot precursors, Combustion and Flame 156 (3) (2009) 588 – 607.
URL `http://www.sciencedirect.com/science/article/pii/S0010218008003957`

[47] M. Mehl, W. J. Pitz, C. K. Westbrook, H. J. Curran, Kinetic modeling of gasoline surrogate components and mixtures under engine conditions, Proceedings of the Combustion Institute 33 (1) (2011) 193 – 200.
URL `http://www.sciencedirect.com/science/article/pii/S1540748910000787`

[48] W. Ji, P. Zhang, T. He, Z. Wang, L. Tao, X. He, C. Law, Intermediate species measurement during iso-butanol auto-ignition, Combustion and Flame 162 (2015) 3541–3553.

[49] D. Davidson, R. Hanson, Fundamental kinetics database utilizing shock tube measurements. Volume 4. ignition delay time measurements, Tech. rep., Stanford University (2014).